

Deuterium Depletion Inhibits Cell Proliferation, RNA and Nuclear Membrane Turnover to Enhance Survival in Pancreatic Cancer

László G. Boros^{1,2}, Ildikó Somlyai³, Beáta Zs. Kovács³, László G. Puskás⁴, Lajos I. Nagy⁴, László Dux⁵, Gyula Farkas⁶, and Gábor Somlyai³ 

Abstract

The effects of deuterium-depleted water (DDW) containing deuterium (D) at a concentration of 25 parts per million (ppm), 50 ppm, 105 ppm and the control at 150 ppm were monitored in MIA-PaCa-2 pancreatic cancer cells by the real-time cell impedance detection xCELLigence method. The data revealed that lower deuterium concentrations corresponded to lower MIA PaCa-2 growth rate. Nuclear membrane turnover and nucleic acid synthesis rate at different D-concentrations were determined by targeted [1,2-¹³C₂]-D-glucose fate associations. The data showed severely decreased oxidative pentose cycling, RNA ribose ¹³C labeling from [1,2-¹³C₂]-D-glucose and nuclear membrane lignoceric (C24:0) acid turnover. Here, we treated advanced pancreatic cancer patients with DDW as an extra-mitochondrial deuterium-depleting strategy and evaluated overall patient survival. Eighty-six (36 male and 50 female) pancreatic adenocarcinoma patients were treated with conventional chemotherapy and natural water (control, 30 patients) or 85 ppm DDW (56 patients), which was gradually decreased to preparations with 65 ppm and 45 ppm deuterium content for each 1 to 3 months treatment period. Patient survival curves were calculated by the Kaplan-Meier method and Pearson correlation was taken between median survival time (MST) and DDW treatment in pancreatic cancer patients. The MST for patients consuming DDW treatment (n = 56) was 19.6 months in comparison with the 6.36 months' MST achieved with chemotherapy alone (n = 30). There was a strong, statistically significant Pearson correlation (r = 0.504, p < 0.001) between survival time and length and frequency of DDW treatment.

Keywords

deuterium-depleted water (DDW), NAD(P)H synthesis, oxidative pentose cycle, median survival time (MST), unresectable pancreatic cancer, peritoneal tumor infiltration

Received December 18, 2020. Received revised December 18, 2020. Accepted for publication January 28, 2021.

¹ Department of Pediatrics, Harbor-UCLA Medical Center and The Lundquist Institute for Biomedical Innovation, Torrance, CA, USA

² SIDMAP, LLC, Los Angeles, CA, USA

³ HYD LLC for Cancer Research and Drug Development, Budapest, Hungary

⁴ AVIDIN Ltd, Szeged, Hungary

⁵ Department of Biochemistry, Albert Szent-Györgyi Medical University, University of Szeged, Szeged, Hungary

⁶ Department of Surgery, Albert Szent-Györgyi Medical University, University of Szeged, Szeged, Hungary

Corresponding Author:

Gábor Somlyai, HYD LLC for Cancer Research and Drug Development, 1118 Budapest, Villányi út 97. Hungary.

Email: gsomlyai@hyd.hu



Creative Commons Non Commercial CC BY-NC: This article is distributed under the terms of the Creative Commons Attribution-NonCommercial 4.0 License (<https://creativecommons.org/licenses/by-nc/4.0/>) which permits non-commercial use, reproduction and distribution of the work without further permission provided the original work is attributed as specified on the SAGE and Open Access pages (<https://us.sagepub.com/en-us/nam/open-access-at-sage>).

Introduction

Pancreatic cancer is a rapidly developing disease with poor prognosis and it is the fourth leading cause of cancer-related deaths in the Western Hemisphere. Surgical extirpation of localized disease in a small segment of patients receiving radiotherapy and concurrent 5-fluorouracil-based chemotherapy prolongs overall survival to 1.8 years.¹ Ninety-five percent of patients, who are diagnosed at stage III or IV of the disease with unresectable tumors, expect only an average of 4 to 6 months to live.² Patients with unresectable tumors have only a 20% chance of surviving 1 year following diagnosis and treatment with single-agent chemotherapy.³ Current major adjuvant treatment strategies include a second agent, either a cytotoxic or targeted agent, to gemcitabine, and combined chemoradiotherapy regimens have also been explored to improve overall survival, with limited success.² Advanced pancreatic tumors can be reduced into resectable states by the use of regional chemotherapy that brings about improvements in overall survival. Approximately 80% of pancreatic cancer patients have no option for curative resection at the time of diagnosis.⁴

A number of biological agents modulating different signal transduction pathways are currently in clinical development, inhibiting angiogenesis and targeting epidermal growth factor receptor, cell cycle, matrix metalloproteinases, cyclooxygenase-2, mammalian target of rapamycin, or proteasome, but only a few of them are approved for use in clinical practice with limited benefit-to-cost ratios.⁵ Borderline resectable pancreatic carcinoma has a high risk for margin-positive resection. There is a consensus that such cancers should be treated with neoadjuvant chemotherapy and/or chemoradiotherapy before resection. An extended surgical approach including resection of the superior mesenteric/portal vein and/or the hepatic artery should be performed when necessary.⁶ Although margin-negative resection is achieved in 98% of borderline resectable pancreatic cancer, survival rate for the patients with borderline resectable disease was lower than the rate for those with resectable pancreatic cancer due to a higher incidence of peritoneal and distant recurrence.⁷

Restored mitochondrial fumarate hydratase activity has been shown to eliminate aggressive kidney cancer xenograft growth⁸ by switching NADPH production from pentose cycle back to the mitochondrial matrix.⁹ The oncogenic up-regulation of pentose cycle metabolism and NADPH yielding an irreversible oxidative arm^{10,11} is a well-established metabolic hallmark of human cancer, as demonstrated by targeted [1,2-¹³C₂]-D-glucose fate associations studies in lung,¹² colon¹³ and pancreatic cancer.¹⁴ The recognition that Gleevec treatment by restoring mitochondrial fatty acid oxidation results in profound intracellular metabolic changes that bring devastating consequences for the survival/proliferation of leukemia cells of the Bcr-Abl-positive myeloid lineage,^{15,16} confirm the role of mitochondria in cell cycle regulation.

A novel, submolecular approach to tumor cell physiology and metabolism can provide explanation to understand the role of mitochondria in the control of cell division. Two stable

isotopes of hydrogen, protium (H) and deuterium (D) differ in their physicochemical nature.¹⁷⁻¹⁹ Increasing evidence suggests that D plays a key role in cell proliferation. Consistent with this, the effect of low deuterium in controlling cell proliferation is already verified in numerous biological systems.²⁰⁻²⁷ The growth rate of tumor cells is significantly inhibited in culture media prepared with deuterium-depleted water (DDW), and DDW treatment of mice xenotransplanted with MDA-MB-231, MCF-7 human breast adenocarcinomas, or PC-3 human prostate tumors resulted in complete or partial tumor regression.^{20,21} The apoptosis-triggering effect of DDW was demonstrated both *in vitro*²¹ and *in vivo*.²² When laboratory animals are exposed to the chemical carcinogen agent DMBA and expression of c-myc, Ha-ras, and p53 genes are induced, replacement of drinking water with DDW suppressed the expression of these genes.²⁸ In addition, DDW significantly inhibited the proliferation of A549 human lung carcinoma cells *in vitro*, while H460 lung tumor xenografts in laboratory mice showed a 30% growth regression.²³ Cancer cells are extremely sensitive to D-depletion, which can cause tumor necrosis induced by ROS (reactive oxygen species).¹⁷ Recent studies confirmed that D is a natural cell growth regulator that controls mitochondrial oxidation-reduction balance.¹⁷⁻¹⁹

The anti-cancer effect of D-depletion has already been confirmed in a double-blind, randomized, 4-month-long phase II clinical trial on prostate cancer, and the extended follow-up suggests that D-depletion readily delays the progression of the disease.²⁹ D-depletion, in addition to the conventional treatments, improves mean survival time in lung cancer³⁰ even in an advanced disease, complicated by distant brain metastases.²⁴ In breast cancer patients, DDW treatment in combination with, or as an extension of, conventional therapies, significantly improved survival in advanced disease and was also effective in the prevention of recurrences in early-stage breast cancer.³¹

Herein we report that D-depletion in water alone inhibits MIA PaCa-2 pancreatic cancer cell growth *in vitro* by controlling NADPH-dependent reductive synthesis via the oxidative pentose cycle and that the decrease of serum deuterium after the consumption of DDW in addition to conventional therapies offers a 3-fold extension in MST in patients with advanced pancreatic cancer.

Materials and Methods

Production of Deuterium-Depleted Water (DDW)

DDW containing Deuterium (D) at concentrations of 25 parts per million (ppm)³¹ is fractionated based on the different volatility of HDO and D₂O compared to light water (H₂O), which has 150 ppm D in HDO and D₂O form (heavy water). The proper D-concentration for different experiments was prepared by mixing DDW with 25 ppm D-concentration with distilled water of 150 ppm D-concentration. At the boiling point of normal water, the steam in equilibrium with the liquid phase contains approximately 2.5% less DHO (semi-deuterated

water). Industrial quantities of DDW is obtained by repeating evaporation steps in vacuumed distillation towers and by European Standards the deuterium content of water is decreased commensurate with the tray number of the distillation tower. For the current study, D-concentration in culture media, drinking water and venous blood serum were determined by mass spectrometry (Finnigan delta plus XP, using BTW XV standards) with ± 1 ppm precision and reported in reference to the Vienna standard of mean oceanic water (<150 ppm).^{32,33} Repeated blood D-concentration measurements were also performed in serum and correlated with daily deuterium intake (including drinking water and food) of 40 ppm, 65 ppm and 100 ppm water. The Michaelis–Menten kinetics of serum and interstitial water pool deuterium saturation and exchange in response to decreasing deuterium intake in water by a patient volunteer was determined.

Culture Media and Cell Lines

Media with increasing D-concentrations were prepared using 6.68 g DMEM (1000 ml stock powder; Gibco BRL, Carlsbad, CA, USA), containing penicillin (50 IU/ml), streptomycin (50 mg/ml), 10% fetal bovine serum (FBS) and 2% horse serum. The final volume of DDW preparations was allocated as fractions in distilled water containing D at a concentration of 150 ppm, by mixing (vol/vol) with the DDW stock containing D at a concentration of 24 ppm. Culture media were filtered using Acrodisc Premium 25 mm syringe filters with 0.2 μm GHP membrane (Pall Life Sciences, NH, USA). The 2-stock media, i.e.: 24 ppm and 150 ppm D, were mixed to yield 50 ppm and 105 ppm D-concentration for the dose-dependent proliferation studies. Cells were starved with FBS depletion overnight. For real-time cell adhesion assay, MIA PaCa-2 cells were seeded at a density of 11000 cells per well into 96-well E-plates and maintained in a humidified atmosphere cell culture cabinet with 95% filtered air and 5% CO₂.

Real-Time Cellular Impedance Analysis Using the xCELLigence System

Cell growth was monitored with the real-time electronic impedance sensing xCELLigence System (RT-CES, Acea-Roche, Basel, Switzerland).³⁴ Cytotoxic effects of DDW containing D at a concentration of 25 ppm, 50 ppm, 105 ppm and the control (150 ppm) as single treatments or in combination with cisplatin (Selleckchem, Avidin Ltd, Hungary, Szeged) at a concentration of 20 μM , 40 μM or 60 μM were tested in MIA PaCa-2 (CRL-142, American Type Culture Collection—ATCC) human pancreatic carcinoma cells. Cisplatin was freshly diluted in a concentration of D matching DMEM culture media. The cells were given the freshly prepared cisplatin and volume equivalent media prepared with DDW at the same time as DDW control cultures. The RT-CES 96-well E-plate was coated with gelatin and then washed twice with PBS. Growth media were then gently dispensed into each well of the 96-well E-plate for background readings by the RT-CES

system prior to addition of cell suspension at a density of 11000 cells in each well. Impedance reading plate holding devices containing the cell suspension were kept at 37 °C in a CO₂ incubator overnight prior to treatment with DDW and/or cisplatin. Cell growth was monitored for 72 h by recording electrical impedance every 5 minutes. The dimensionless parameter termed Cell Index (CI) was derived as relative change in measured electrical impedance of DDW cultures relative to the control 150 ppm impedance, which reflects viability of treated cells as well as their count, respectively.

Targeted [1,2-¹³C₂]-D-Glucose Fate Association Study

All reagents were purchased from Sigma-Aldrich (St. Louis, MO) unless otherwise stated. All experiments were conducted in triplicate. Twenty-four hours prior to DDW treatment and metabolomics study, 2 x 10⁶ MIA-PACA, H449 or MCF-7 positive control cells were grown in T-75 cm² culture flasks with glucose and sodium pyruvate-free DMEM containing 10% FBS, 1% penicillin/streptomycin, 180 mg/dL, of which 50% of total final glucose was derived from the [1,2-¹³C₂]-D-glucose tracer (Isotec, Miamisburg, OH). The tracer was added to the media for all cells for 72 hours. Media and trypsinized cell lysates were collected and frozen at -80°C until analysis.

Product Extraction and Derivatization

Extraction and derivatization procedures for glucose, cholesterol, fatty acids, lactate, CO₂ and glutamate were previously published for targeted tracer fate association matrices.³⁵ Sterols and fatty acids were extracted by saponification of Trizol (500 μL , Invitrogen, Carlsbad, CA) cell extract after removal of the upper glycogen- and RNA-containing supernatant using 30% KOH and 70% ethanol (300 μL each) for 2 hours.³⁶ Sterol extraction was performed using 5 mL petroleum ether (EMD, Gibbstown, NJ) with repeated shaking for 20 seconds 3 times. The molecular ion of cholesterol was monitored at the m/z 386 ion cluster. Fatty acids were extracted by further acidification using 6 N hydrochloric acid to pH below 2.0 and repeated vortexing with 5 mL petroleum ether. Fatty acids (methyl-palmitate; C16:0) were monitored at m/z 270 using canola oil as positive control and methyl-lignocerate (C24:0) was monitored at m/z382. The enrichment of acetyl units in media and cell pellet palmitate in response to 100 ppm, 50 ppm and 25 ppm DDW treatments was determined using the mass isotopomer distribution analysis (MIDA) approach. Acetyl-CoA and fractions of new synthesis were calculated from the m4/m2 ratio using the formula $m4/m2 = (n-1)/2 \bullet (p/q)$, where n is the number of acetyl units, p is the ¹³C-labeled precursor acetate fraction and q is the ¹²C-labeled natural acetate fraction ($p+q = 1$).^{37,38}

For glucose extraction, 500 μL each of 0.3 N barium hydroxide and 0.3 N zinc sulfate were added to 100 μL media. Samples were vortexed and centrifuged for 15 min at 10,000 rpm. Supernatant was dried on air overheat and were

derivatized by adding 150 μL hydroxylamine solution and incubated for 2 h at 100°C followed by addition of 100 μL of acetic anhydride. Samples were incubated at 100°C for 1 h and dried under nitrogen overhead as previously described in the fatty acid derivatization section. Ethyl acetate (200 μL) was added. Peak glucose ion was detected at m/z 187 cluster.

Lactate was extracted from media through acidification of 100 μL media with HCl and addition of 1 mL of ethyl acetate. The resulting aqueous layer was dried under nitrogen overhead and derivatized using lactate standard solution as positive control. 200 μL of 2,2-dimethoxypropane was added followed by 50 μL of 0.5 N methanolic HCl. Samples were incubated at 75°C for an hour. 60 μL of *n*-propylamine was added and samples were heated for 100°C for an hour followed by addition of 200 μL dichloromethane. Heptafluorobutyric anhydride (15 μL) was added followed by 150 μL of dichloromethane and samples were subjected to GC/MS. M1 and m2 lactate were differentiated to distinguish the pentose phosphate flux from anaerobic glycolysis and the ion cluster at m/z 327 (electron impact ionization) was examined.³⁹

¹³CO₂ Assay for CO₂ was generated by adding equal volumes (50 μL) of 0.1 N NaHCO₃ and 1 N HCl to spent media and ¹²CO₂/¹³CO₂ ion currents were monitored and calculated from the m/z 44 and m/z 45 peak intensities, respectively, using ¹³CO₂/¹³CO₂ of cell culture cabinet's CO₂ tank as the reference ratio for ¹³CO₂ calculations.

Gas Chromatography/Mass Spectrometry

Agilent 5975 Inert XL Mass Selective Detector connected to HP6890 N Network gas chromatograph was used to detect mass spectral data under the following settings: GC inlet 230°C, MS source 230°C, MS Quad 150°C.⁴⁰ For media CO₂, glucose and lactate analyses, an HP-5 column (30 m length x 250 μm diameter x 0.25 μm thickness) was used while a DB-23 column (60 m length, 250 μm diameter x 0.15 μm thickness) was used for fatty acid measurements.

Statistics

Mass spectral analyses were obtained by consecutive and independent injections of 1 μL sample using an autosampler with optimal split ratios for column loading ($10^6 > \text{abundance} > 10^4$ abundance). Ion currents were accepted for spectra processing if the standard sample deviation was below 5% of the normalized peak intensity (integrated peak area of ion currents; 100%) among repeated injections. Data download was performed in triplicate manual peak integrations using modified (background subtracted) spectra under the overlapping isotopomer peaks of the total ion chromatogram (TIC) window displayed by the Chemstation (Agilent, Palo Alto, CA) software by spectral chemistry technicians, who were blinded to sample identities, blanks and natural ¹³C abundance internal standard study samples. A 2-tailed independent sample t-test was used to test for significance ($p < 0.05$, $p < 0.01$) between control

(150 ppm DDW) and the treated groups (100 ppm, 50 ppm and 25 ppm D for DDW responsive metabolic flux surrogates).

Clinical Study Design and Eligibility Criteria

A total of 86 (36 males and 50 females) patients with histologically confirmed pancreatic carcinoma were continually enrolled (DDW group = 56, control group = 30) from March 1995 to January 2020. Two of these patients, 1 female and 1 male were operated before entering the study, the other patients were inoperable. Patients were evaluated on approved EU compliant Institutional Review Board (IRB) protocol (Clinical Trials Identifier: HYDPACA1995-2020 for this report; Principal Investigator: Somlyai G. PhD) and for surgically evaluated 150 ppm DDW controls (SZOTE; Principal Investigator: Farkas jr. Gy. MD, PhD). Regarding the length of DDW treatment, patients who continued taking DDW for at least 91 days were eligible. Fifty-six (22 males and 34 females) patients met the inclusion criteria of this report in the DDW group, and their clinical progression was retrospectively evaluated. For the DDW group daily water intake of all patients was replaced with DDW, which was integrated in the conventional treatment regimens, as patients were administered DDW orally, *ad libitum*, in addition to the conventional treatment regimen. These patients were continuously updated with, aware of, and provided access to all available information and publications regarding the DDW treatment that they consented to. DDW treatment started with 85 ppm D, which was gradually (every 1-3 months) decreased to preparations with 65 ppm and 45 ppm for 30 to 90 days (1 to 3 months). The endpoint of the study was overall survival based on vital statistics. We used Kaplan-Meier survival estimates. Explanatory variable was the time from diagnosis to end to follow-up in months. Outcome variable was death. For correlation analysis, the Pearson method was used. Variables were DDW treatment in days and survival time in days. The calculations were performed by AdwareResearch Partner.

Disease Characteristics in the 56 DDW-Treated Pancreatic Cancer Patients

Patients had already been diagnosed with advanced stage IV pancreatic cancer before they entered the DDW study.

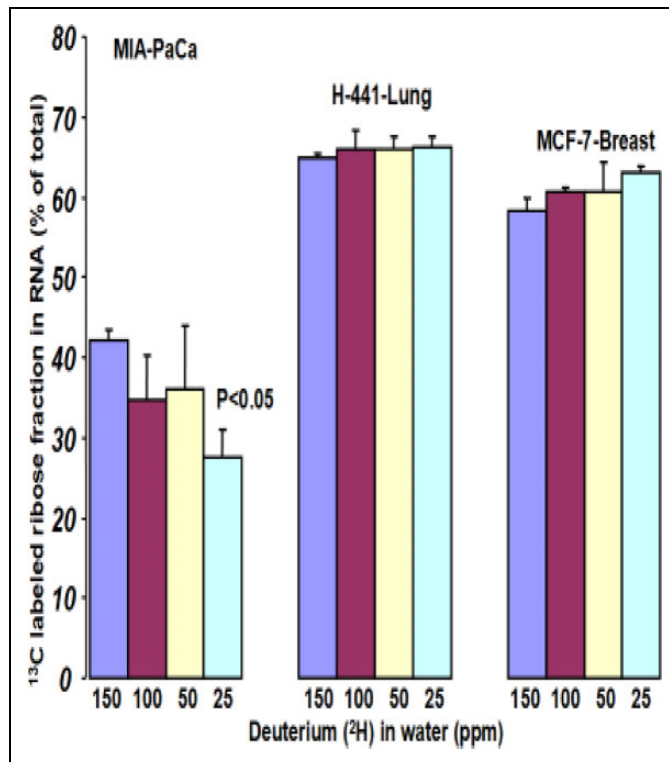
26 patients had metastatic pancreatic cancer. Different types of metastases were detected in 18 patients (69.2%), mostly in the liver. All patients underwent conventional treatments with chemotherapeutic agents except one 69-year-old female patient. The majority of patients were treated with standard intravenous gemcitabine, which was combined with 5-fluorouracil in 4 cases. Cisplatin was used as the primary chemotherapeutic drug in 3 patients.

The median age of the 56 DDW-treated patients was 62.0 years. Median duration of the treatment with DDW was 7.3 months (85 ppm, 65 ppm and 45 ppm regimen (DDW)). The treatment period showed a high standard deviation (SD: 8.18 months), because 12 patients (21%) consumed DDW

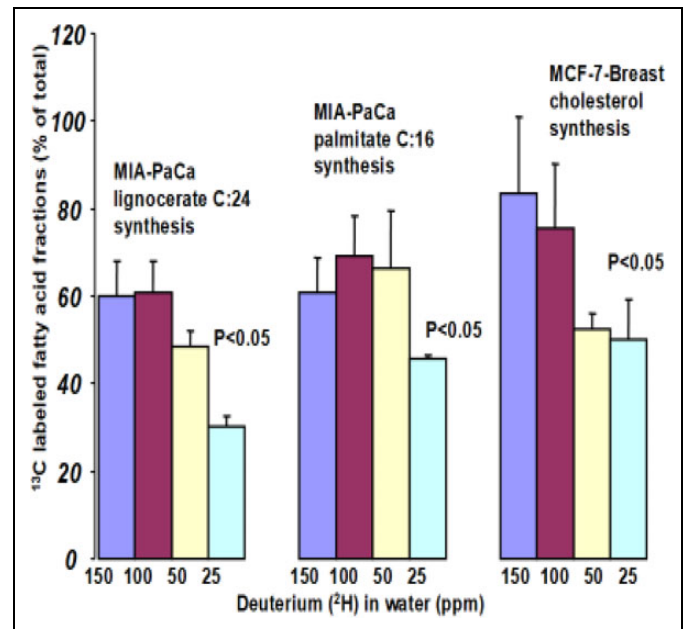
Table 1. Descriptive Statistics of the 56 DDW Treated Patients With Pancreatic Cancer.

Variable	Median	Mean	Standard deviation of mean	Cumulative time
DG_to_DDWstart	1.7 months	6.1 months	12.2 months	27.9 years
Low DDW	7.3 months	10.2 months	8.18 months	47.1 years
DG_to_Flwup	13.1 months	20.7 months	22.2 months	95.3 years
DDWstart_to_Flwup	8.4 months	14.6 months	17.1 months	67.4 years

L/E = 31/25.

**Figure 1.** Targeted [1,2-¹³C₂]-D-glucose fate associations show decreased RNA ribose turnover in Mia-PaCa cells after DDW treatment, whereby the more differentiated H441 (lung) and MCF-7 (breast) cells showed no response in ribose ¹³C turnover in this 72 hours ¹³C labeling study. (n = 3; +SD).

for an extended period, more than 1 year, upon clinical improvement, with the longest treatment periods reaching up to 1.2 and 3.2 years. Follow-up period from the diagnosis (DG to Flwup) was also longer in comparison with other clinical reports on advanced pancreatic cancer, DG_to_Flwup was 13.1 months (SD: 22.2 months). Patients started the DDW treatment at different time points at their consent after the diagnosis, which was recorded, and the median lengths between diagnosis and entering the trial (DG_to_DDWstart) was 1.7 months (SD: 12.2 months). When data sheets were closed in order to meet study deadline objectives (January 2020) for standard matrix diagnostics, data processing and abstracting, 31 patients were still alive (L/E = 31/25) and were offered continued DDW treatment. Therefore these patients are included in this report with at least their applicable (*at least*) mean survival time upon study termination (Table 1).

**Figure 2.** Targeted [1,2-¹³C₂]-D-glucose fate associations show decreased limited nuclear membrane fatty acid lignocerate (C24:0) synthesis and palmitate (C16:0) synthesis in MIA-PaCa cells.

Disease Characteristics in the 30 Control Pancreatic Cancer Patients Ingesting Normal Water (150 ppm)

The median age of the 30 control, natural deuterium-containing water-consuming patients was 65.9 years (SD = 9.05 years) (Female: n = 16, Average age: 67 years, SD = 9.24 years; Male: n = 14, Average age: 64.3 years, SD = 8.9). When control patients were explored for potential surgical resection, disseminated diseases with liver and lymph node metastases were observed and multiple lymph node biopsies were obtained without additional surgical intervention. Histology in all cases confirmed pancreatic adenocarcinoma and all patients received standard treatment with gemcitabine (Gemzar 1000 mg/m² as an intravenous infusion) combined with 5-fluorouracil consistent with the EU gastrointestinal adenocarcinoma disease management protocol.

Results

In vitro growth inhibition by deuterium-depleted water (DDW) alone or in combination with cisplatin in MIA PaCa-2 pancreatic cancer cells

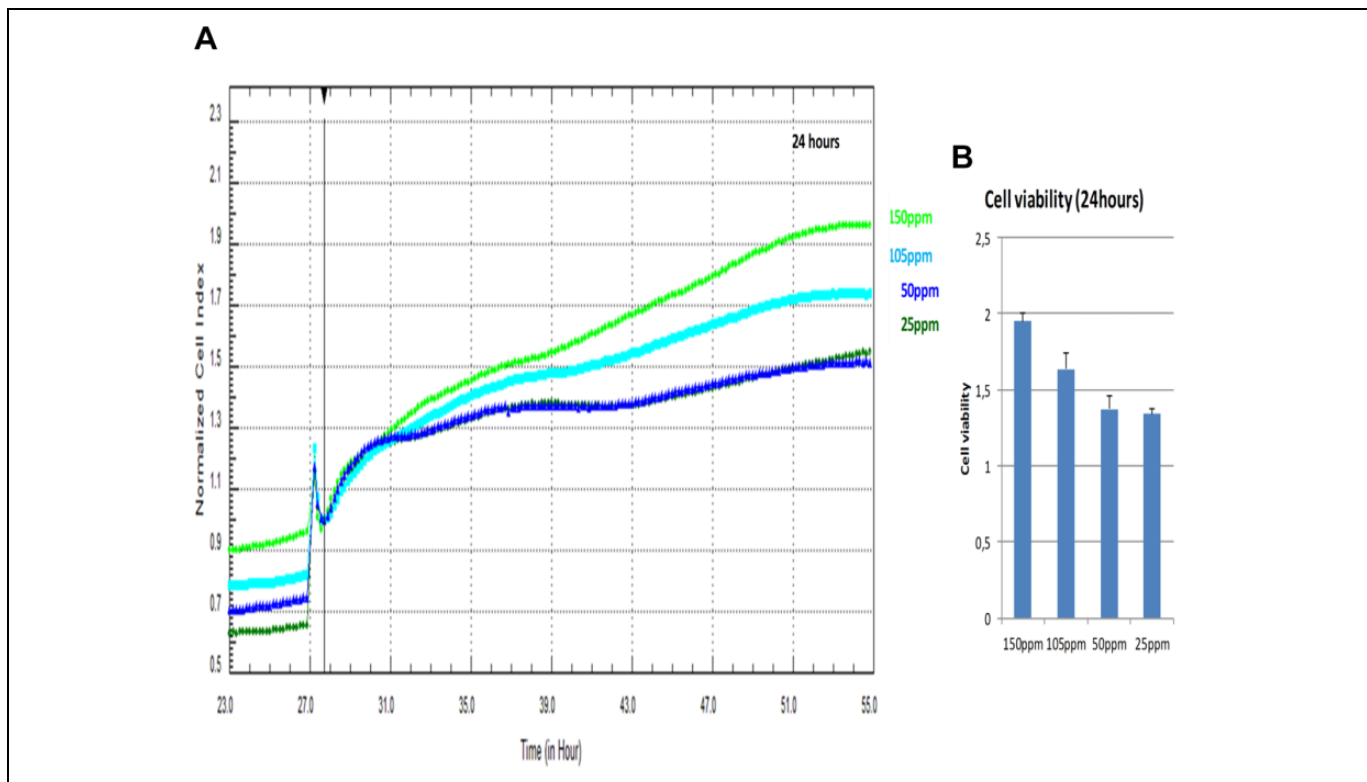


Figure 3. (a) Decreased cell impedance and count (Cell Index) after treatment with low concentrations of D (25 ppm, 50 ppm or 105 ppm) in MIA PaCa-2 pancreatic cancer cells in a growth curve after priming for 24 hours, then allowing to propagate up to 55 hours. (b) MIA-PACA-2 viability after 24 hours of DDW treatment in comparison with control cultures as indicated on the Y-axis. Natural D concentration (150 ppm) was used for control in the first 24 hours ($n = 3$ +SD; * $p < 0.05$ in DDW treated cultures in comparison with 150 ppm control).

Targeted $[1,2-^{13}\text{C}_2]$ -D-Glucose Fate Associations

Targeted $[1,2-^{13}\text{C}_2]$ -D-glucose fate associations indicated that new RNA ribose synthesis and turnover decreased in Mia-PaCa cells after DDW treatment (Figure 1), which was associated with limited nuclear membrane fatty acid lignocerate (C24:0) and palmitate (C16:0) syntheses. MCF-7 breast cancer cells also showed a metabolic response, whereby nuclear membrane cholesterol synthesis was decreased (Figure 2).

Culture media $[3-^{13}\text{C}_1]$ -DL-lactate and $[2,3-^{13}\text{C}_2]$ -DL-lactate ratios, produced from the $[1,2-^{13}\text{C}_2]$ -D-glucose tracer via the oxidative branch of the pentose cycle in the expense of the hexose phase of the glycolytic flux showed a significant decrease in glucose-6-P dehydrogenase (G6PDH) flux and NADPH production from the 5.45 ($n = 3$; SD = 0.17) control value to 4.75 ($n = 3$; SD = 0.16) 100 ppm DDW, 4.75 ($n = 3$; SD = 0.22) 50 ppm DDW and 4.82 ($n = 3$; SD = 0.19) 25 ppm DDW treatment, respectively.

Cell Growth Inhibitory Effect

The cell growth inhibitory effect of D-depletion on the MIA PaCa-2 pancreatic cancer cell line was investigated using the real time, non-label system of xCELLigence RTCA. Cells were treated with DDW containing deuterium at a concentration of

25 ppm, 50 ppm or 105 ppm and the impedance Cell Index (CI) was plotted for each treatment. Control measurement was carried out by adding D to cells at the natural concentration of 150 ppm. Lower D-concentrations showed dose-dependent decrease in CI compared to water containing D at 150 ppm (Figure 3).

The growth inhibitory effect of DDW was confirmed by the fact that MIA PaCa-2 cells are resistant to gemcitabine and consistent with this, the combined treatment with gemcitabine (60 μM) and DDW did not result in further inhibition of previously observed cell growth or cell viability achieved with DDW. In other words, CI values did not differ significantly from the values that were measured with decreasing deuterium concentrations without gemcitabine as shown in Figure 3.

Cytostatic Effect

The cytostatic effect of 20 μM , 40 μM or 60 μM cisplatin in MIA PaCa-2 cells was evident by the dose-dependent decrease of CI values during the real-time cell impedance test using D at the 50 ppm (Figure 4a). Treatment with 20 μM cisplatin in cell medium containing 50 ppm and 25 ppm D resulted in significantly lower CI values at 24hs than that with 150 ppm or 50 ppm DDW alone (Figure 4b).

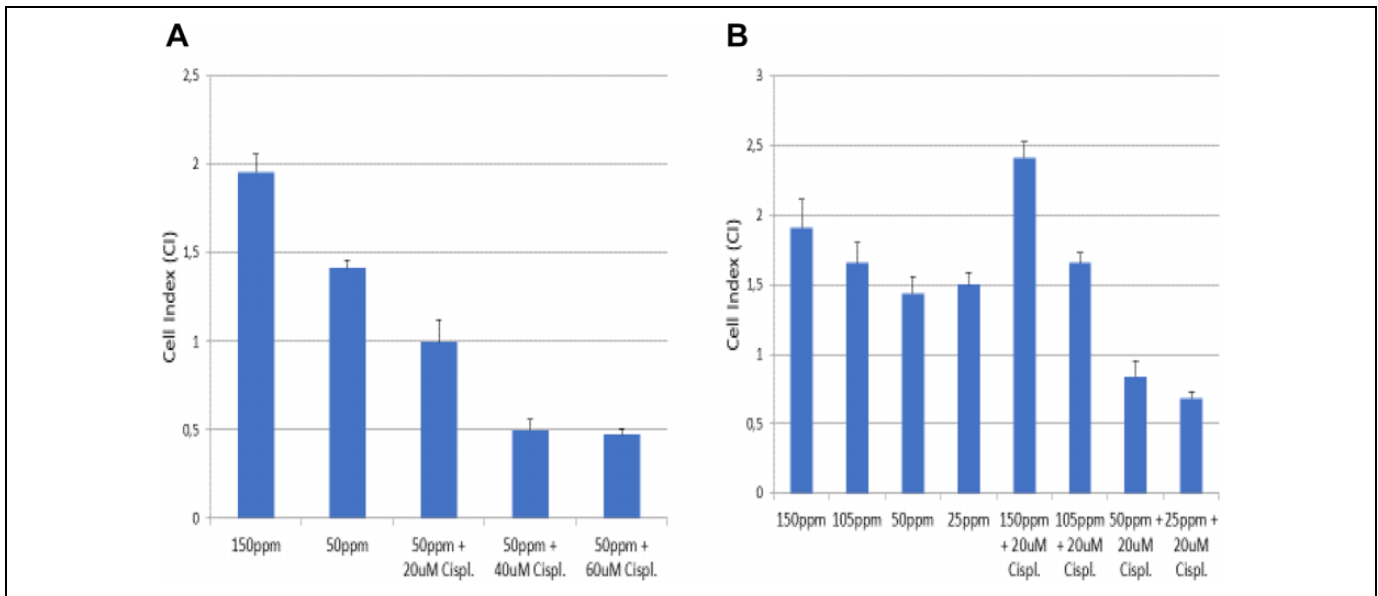


Figure 4. (a) Cisplatin at 20 μ M, 40 μ M and 60 μ M concentration, for 24 h inhibited cell viability of MIA PaCa-2 pancreatic cells dose-dependently, compared to CI values measured after treatment with 50 ppm D-concentration. ($n = 3 +SD$; $*p < 0.05$ in DDW treated cultures in comparison with 150 ppm and 50 ppm of D; $\#p < 0.05$ in DDW treated cultures in comparison with 20 μ M cisplatin). (b) Cisplatin at 20 μ M concentration for 24 h inhibited cell viability of MIA PaCa-2 pancreatic cells dose-dependently after treatment with 105 ppm, 50 ppm and 25 ppm of D, compared to CI values to control (150 ppm + 20 μ M cisplatin) ($n = 3 +SD$; $*p < 0.05$ in DDW and cisplatin-treated cultures in comparison with 150 ppm and 20 μ M cisplatin-treated culture)

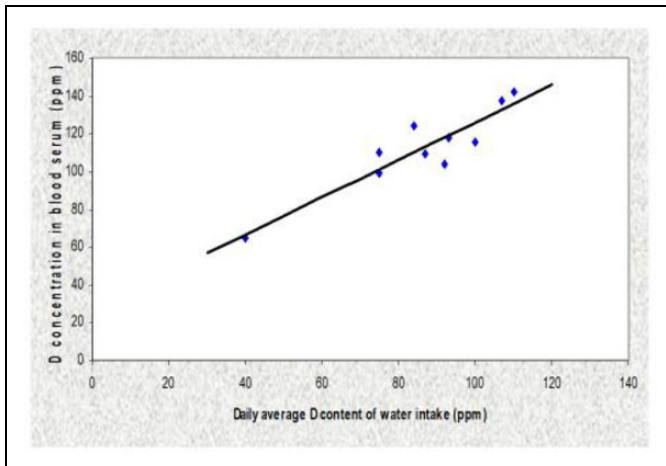


Figure 5. Scatterplot of daily DDW-intake (including drinking water and food) for several weeks or months and serum D-concentrations. Slope and intercept: $y = 0.9873x + 27.17$. ($n = 10$; $R^2 = 0.85$).

Regression Statistics Between Average Daily DDW-Intake

Regression statistics between average daily DDW-intake (including drinking water and food) for several weeks or months and serum D-concentrations ($n = 10$; Figure 5) showed a $y = 0.9873x + 27.177$ slope and intercept with a very high >0.8 ($R^2 = 0.8497$) positive correlation coefficient between dietary deuterium content (degree of deuterium-depletion) and that of serum.

Michaelis–Menten kinetics of serum and interstitial water pool saturation and exchange in response to lowered D-intake

of 10 different cancer patient volunteers showed the equilibrium concentration after DDW-consumption. The data on Figure 5 show deuterium (precursor enrichment) in serum and interstitial fluid via deuterium exchange after a period of time of any given DDW sample consumption as shown on the X-axis.

Pearson correlation was measured between survival times and DDW treatment in pancreatic cancer patients (Figure 6).

We found a strong, statistically significant correlation between survival time and length of DDW treatment. ($r = 0.504$, $p < 0.001$).

DDW Consumption Increases MST

Calculations of the MST by the 56 DDW-Consuming Patients

Deuterium depletion increased MST in all 56 patients who, in addition to the conventional cytostatic treatments for pancreatic cancer, also underwent treatment with DDW. The MST from diagnosis (Figure 7) was on average 19.6 months in the DDW-treated cohort.

The MST in the control group with 30 patients was 6.88 months in females ($n = 16$; $SD = 2.52$) and 5.86 months in males ($n = 14$; $SD = 2.03$).

Calculations of the MST Using Different Parameters, Cohort by Gender, Metastasis, Age and Weight

The MST was 21.467 months (95% CI: 12.031-30.902) in the female subgroup ($n = 34$) and 15.167 (95% CI: 7.824-22.509) in the male subgroup ($n = 22$).

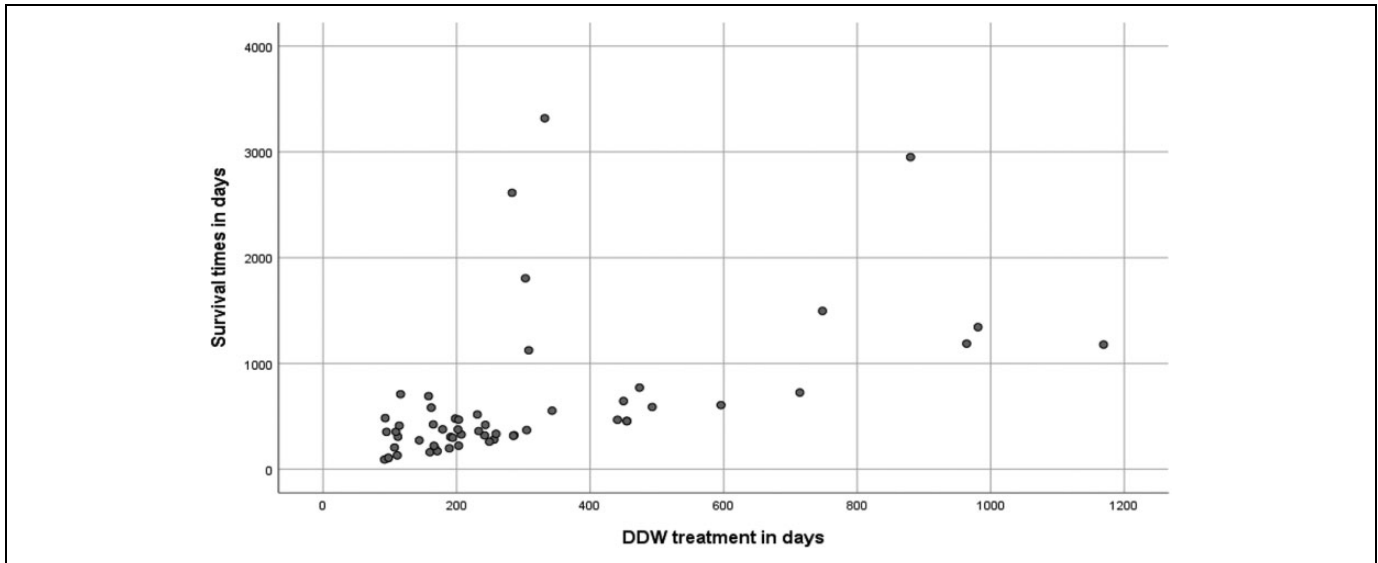


Figure 6. Pearson correlation between survival time in days and DDW treatment in days for 56 pancreatic cancer patients.

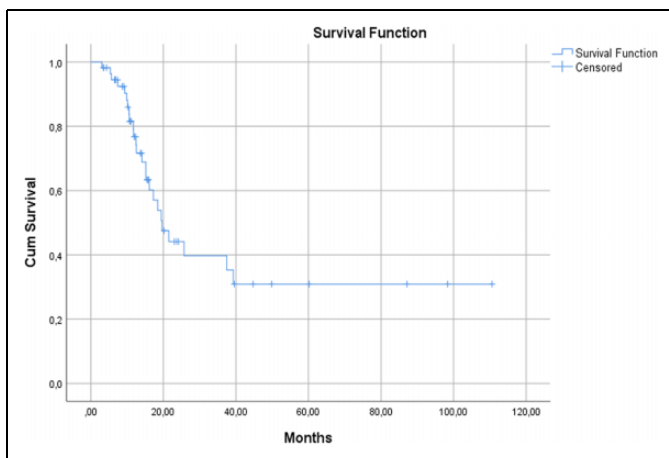


Figure 7. Calculation of MST in 56 pancreatic cancer patient cohort (95% CI: 14.252-24.948).

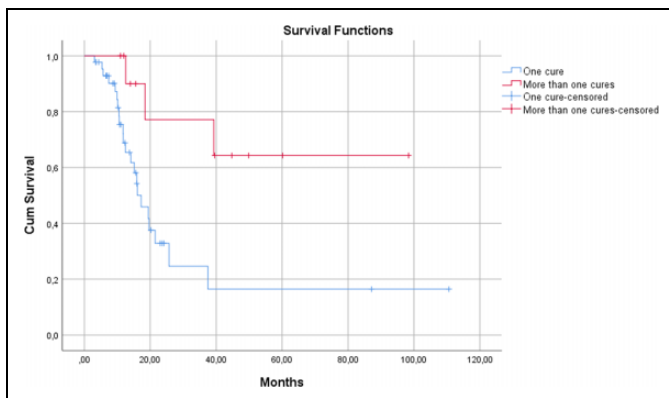


Figure 8. MST in the 56 pancreatic cancer patient cohort calculated using the number of cures.

The MST was 19.600 months (95% CI: 10.241-28.959) in patients with no metastasis ($n = 30$) and 19.400 (95% CI: 10.281-28.519) in patients with metastasis ($n = 26$).

The MST was 25.700 months (95% CI: 9.612-41.788) in patients younger than 60 years ($n = 23$) and 18.433 (95% CI: 14.187-22.680) in patients older than 60 years ($n = 33$).

The MST was 21.467 months (95% CI: 11.955-30.978) in patients weighing under 70 kgs ($n = 33$) and 17.233 (95% CI: 11.431-23.035) in patients weighing 70 kgs or more ($n = 23$).

Although the differences between the subgroups were not statistically significant, in the comparable subgroups we drew the inference that the changes in MST were very remarkable. The difference was not so large in 1 case, between those patients who had and who not had metastasis.

Calculations of the MST With Statistically Significant Parameters in 56 Pancreatic Cancer Patients Cohort by the Number of Cures

The MST was 17.233 months (95% CI: 12.494-21.973) in patients with only 1 DDW-cure ($n = 44$). MST could not be determined for patients with more than 1 DDW-cure ($n = 12$), the mean survival time was 71.911 months (Figure 8). The difference between the 2 subgroups was statistically significant ($p = 0.010$).

Discussion

Gastrointestinal tract adenocarcinoma malignancies, which are the most common type of pancreatic cancers, are progressive in their clinical appearance. They are often diagnosed at a late stage with severely compromised expectancy and quality of life due to the many serious complications, besides their rapid course. Recent reviews regarding surgical⁴¹ management and

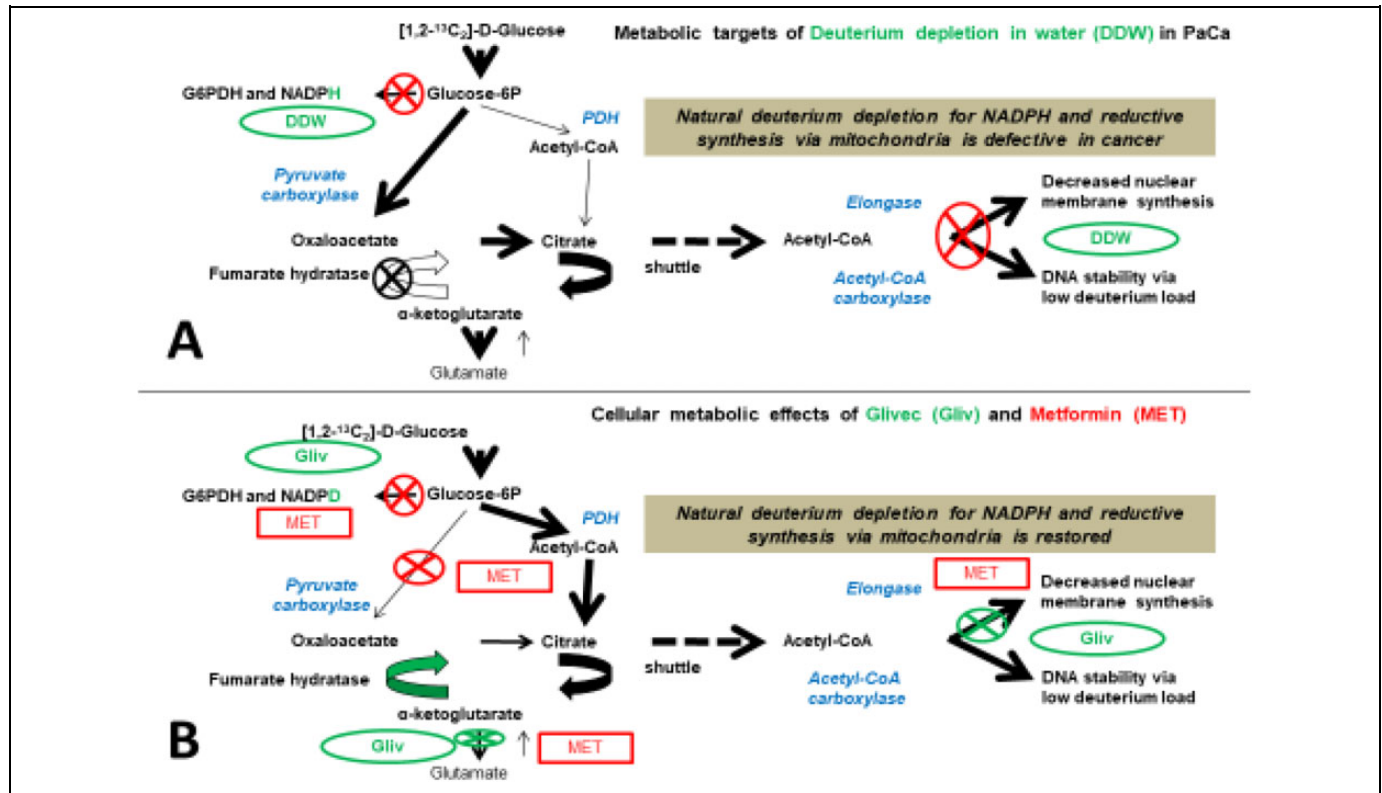


Figure 9. Comparison of metabolic profile changes associated with **A**) deuterium depletion or **B**) Glivec in leukemia and Metformin (MET) in Mia-PaCa cells. In normal cells natural deuterium depletion occurs via mitochondria-dependent NAD(P)H production, a process compromised in all cancer cells. Glivec restores and Metformin improves mitochondrial fatty acid substrate oxidation with TCA cycle turnover and increase fumarate hydratase, hence low deuterium-containing metabolic water recycling for NAD(P)H-driven reductive macromolecule synthesis of the normal mammalian cell. Glivec and Metformin treatment also strongly inhibit the oxidative deuterium loading arm of the pentose cycle from free water (panel **B**). Deuterium depletion in free (drinking) water and the serum of pancreatic cancer patients mimic restored mitochondrial deuterium depletion for reductive synthesis via limiting deuterium load through oncogenic NAD(P)D production in the oxidative arm of the pentose cycle (panel **A**), regardless of compromised mitochondrial activity thus “tricking” tumor cells.

experimental⁴² approaches to address molecular mechanisms admit the lingering of new challenges regarding recurrence, resistance and aggressive/invasive cellular phenotypes. For this report we limited deuterium load via oncogenic NAD(P)H synthesis by the oxidative arm of the pentose cycle, nuclear membrane fatty acid chain elongation and nucleic acid ribose turnover by DDW, which mimic metabolic profiles obtained after Glivec¹⁰ treatment in myeloid leukemia, or after cholesterol and metformin treatment in *in vivo* grown pancreatic cancer (Figure 9).^{36,43}

This work provides a distinct clinical translational proof that providing an extracellular deuterium-depleted water source for tumor cells during defective ketogenic substrate oxidation in the mitochondrial matrix, a process that is being diminished in tumor cells to deplete heavy hydrogen (deuterium) on their own via metabolic water production and recycling, is an efficient integrative therapeutic approach to potentially treat such cancers in the future. Such principle via deuterium-depleting (depleting) metabolic markers has clinically been shown in several independent original contributions involving lung,⁴⁴ rare childhood,⁴⁵ renal cell⁴⁶ and colorectal cancers⁴⁷ with only lacking evidence until now in prostate cancer. The underlying

precise medical biochemistry related mechanism of how defective mitochondria with consequentially diminished low deuterium ketogenic fatty acid substrate oxidation and thus hampered recycling of deuterium-depleted (depleted) metabolic water via TCA cycle hydratase reactions is described elsewhere and herein provided for further reading.^{27,48} Such review of the pertinent literature better positions our results within the growing state of deutenomics art that consistently shows the increased significance of deuterium depletion via natural cellular ketogenic substrate oxidation to preserve normal differentiated cellular phenotype in the above cancers to prevent, reverse or cease cancer formation.

We demonstrated the additive anti-growth inhibitory effects of D-depletion in combination with cisplatin in pancreatic cancer cells, *in vitro*. This is a clear indication that the application of DDW in combination with chemotherapy allows the reduction of chemotherapeutic drug dosing, while keeping similar efficacies. This observation suggests that DDW treatment may possibly attenuate devastating side effects of anticancer drugs at lower, but clinical still efficacious concentrations.

This study recruited and enrolled advanced, pancreatic cancer cases with homogenous surgical staging that reflect an

Table 2. Patient Count Data in Those Patients Who Were Under 70 kg Cohort by Gender.

Gender	Total Number	Number under 70 kg	Percent to overall	Percent to gender
Overall	56	35	62.5	-
Male	22	9	16.1	40.1
Female	34	26	46.4	76.5

Mean \pm SD, n = 56.

advanced late disease. This group of patients has the most limited life expectancy among all cancers, not only that of the pancreas. The study population consisted of 56 patients; whom all, except one 69-year-old woman, underwent chemotherapeutic disease management according to conventional regimens used in the EU. Here we report 19.6 months median MST from diagnosis. These are markedly longer survivals than what retrospective clinical data reveal for advanced pancreatic cancer patient life expectancy.^{49,50} This observation suggests that D-depletion in addition to conventional treatments prolongs survival at an advanced stage more efficiently than any targeted or combined therapy achieved, to date. The one 69-year-old female patient, who elected not to have chemotherapy but deuterium depletion alone, regardless of her advanced disease complicated with a large tumor confined to the head of the pancreas causing obstructive jaundice, liver metastases and diabetes during the follow-up period, still took DDW for 441 days (14.46 months). This data suggests that pharmacological D-depletion below 85 ppm D, followed by further depletion steps to 65 ppm and 45 ppm, respectively, may offer significant delays in disease progression with well-maintained routine daily activities, similar to what is observed in Glivec-treated leukemia patients with similar metabolic targets and mechanisms to control disease progression.

In addition, D-depletion in water or food has exceptionally favorable toxicity profiles by being harmless, and therefore DDW can safely be used according to preclinical and clinical safety evaluations obtained in this study. Patients at advanced, medically complicated disease stages can still be offered DDW, which can readily be integrated into chemotherapy treatment regimens with the clear benefit of controlling epigenetic deuterium loading into DNA and nuclear membrane fatty acids, thus increasing nuclear stability as DDW's primary anticancer property through all extra-mitochondrial NAD(P)H synthesis pathways; particularly that of the direct glucose oxidizing arm of the pentose phosphate pathways, cytoplasmic fumarate hydratase and the serine oxidation glycine cleavage reactions of oncogenic NAD(P)H producing glycolysis with an alternate Warburg effect.⁵¹

The Median survival time for patients consuming DDW treatment (n = 56) was 19.6 months in comparison with the 6.36 months MST achieved with chemotherapy alone (n = 30). MST calculations in different subgroups of 56 patients were taken. Different important records were thoroughly investigated for possible parameters that might influence the outcome,

and the subgroup evaluation was performed based on these aspects.

By parameters of metastasis and age (cut-off: 60 years), we detected differences between the groups. MST was higher in those patients, who had no metastasis compared to patients with metastasis. Furthermore, a big difference was observed in the MST of the age parameter subgroup. MST was much higher in those patients, who were younger than 60 years, compared to patients older than 60 years.

We detected an even bigger difference by gender and weight (cut-off: 70 kgs). MST was significantly higher in the female subgroup, compared to the male subgroup. Furthermore, MST was much higher in patients weighing less than 70 kgs compared to patients weighing more than 70 kgs. Comparing the groups of gender and weight status (Table 2), we could detect a correlation.

Men on average weigh more than women and the lower bodyweight may result in higher DdU in women with the same DDW-intake. This fact also suggests that DdU can be a determinative factor influencing MST.

The other key issue determining the effectiveness of D-depletion was the frequency of DDW applications (single or repeated treatment). Although single DDW treatment extended survival in comparison with published MSTs, repeated DDW treatments resulted in outstandingly long survival times. Patients who took DDW for only 1 treatment period (n=44) had an MST of 17.23 months, whereas patients (n = 12) who took DDW-cures more than once had a mean survival time of 71.91 months.

These results strongly suggest that DDW treatment provided additional benefits to pancreatic cancer patients and had a significant role in delaying progression. Most importantly these findings are in close correlation with the importance of deuterium-depleted metabolic water production via metabolic and nutritional ketosis in the mitochondria of differentiated cells both for the radiological diagnosis and treatment of human cancers.⁵²

Declaration of Conflicting Interests

The author(s) declared no potential conflicts of interest with respect to the research, authorship, and/or publication of this article.

Ethics Statement


Patients were evaluated on approved EU compliant Institutional Review Board (IRB) protocol (Clinical Trials Identifier: HYDPACA1995-2020 for this report; Principal Investigator: Somlyai G, Ph.D.) and for

surgically evaluated 150 ppm DDW controls (SZOTE; Principal Investigator: Farkas jr. Gy, M.D., Ph.D.).

Funding

The author(s) disclosed receipt of the following financial support for the research, authorship, and/or publication of this article: This work was supported by HYD LLC for Cancer Research and Drug Development.

ORCID iD

Gábor Somlyai  <https://orcid.org/0000-0001-9116-6417>

References

1. Miller RC, Iott MJ, Corsini MM. Review of adjuvant radiochemotherapy for resected pancreatic cancer and results from Mayo Clinic for the 5th JUCTS symposium. *Int J Radiat Oncol Biol Phys.* 2009;75(2):364-368. doi:10.1016/j.ijrobp.2008.11.06
2. O'Reilly EM. Adjuvant therapy for pancreas adenocarcinoma. *J Surg Oncol.* 2013;107(1):78-85. doi:10.1002/jso.23230
3. Burris HA, Moore MJ, Andersen J, et al. Improvements in survival and clinical benefit with gemcitabine as first-line therapy for patients with advanced pancreas cancer: a randomized trial. *J Clin Oncol.* 1997;15:2403-2413.
4. Davis JL, Pandalai PK, Ripley RT, Langan RC, Avital I. Expanding surgical treatment of pancreatic cancer: the role of regional chemotherapy. *Pancreas.* 2012;41(5):678-684. doi:10.1097/MPA.0b013e318249955a
5. Zagouri F, Sergentanis TN, Chrysikos D, et al. Molecularly targeted therapies in metastatic pancreatic cancer: a systematic review. *Pancreas.* 2013;42(5):760-773. doi:10.1097/MPA.0b013e31827aedef
6. Cooper AB, Tzeng CW, Katz MH. Treatment of borderline resectable pancreatic cancer. *Curr Treat Options Oncol.* 2013;14(3):293-310. doi:10.1007/s11864-013-0244-6
7. Takahashi H, Ohigashi H, Gotoh K, et al. Preoperative gemcitabine-based chemoradiation therapy for resectable and borderline resectable pancreatic cancer. *Ann Surg.* 2013;258(6):1040-1050. doi:10.1097/SLA.0b013e31829b3ce4
8. Tong WH, Sourbier C, Kovtunovych G, et al. The glycolytic shift in fumarate-hydratase-deficient kidney cancer lowers AMPK levels, increases anabolic propensities and lowers cellular iron levels. *Cancer Cell.* 2011;20(3):315-327. doi:10.1016/j.ccr.2011.07.018
9. Yang Y, Lane AN, Ricketts CJ, et al. Metabolic reprogramming for producing energy and reducing power in fumarate hydratase null cells from hereditary leiomyomatosis renal cell carcinoma. *PLoS One.* 2013;8(8):e72179. doi:10.1371/journal.pone.0072179
10. Boros LG, Lee WN, Cascante M. Imatinib and chronic-phase leukemias. *N Engl J Med.* 2002;347(1):67-68. doi:10.1056/NEJM200207043470116
11. Boros LG, Lee PW, Brandes JL, et al. Nonoxidative pentose phosphate pathways and their direct role in ribose synthesis in tumors: is cancer a disease of cellular glucose metabolism? *Med Hypotheses.* 1998;50(1):55-59. PMID: 9488183.
12. Singh A, Happel C, Manna SK, et al. Transcription factor NRF2 regulates miR-1 and miR-206 to drive tumorigenesis. *J Clin Invest.* 2013;123(7):2921-2934. doi:10.1172/JCI66353
13. Bhalla K, Hwang BJ, Dewi RE, et al. PGC1 α promotes tumor growth by inducing gene expression programs supporting lipogenesis. *Cancer Res.* 2011;71(21):6888-6898. doi:10.1158/0008-5472.CAN-11-1011
14. Boros LG, Lee WN, Go VL. A metabolic hypothesis of cell growth and death in pancreatic cancer. *Pancreas.* 2002;24(1):26-33. PMID: 11741179
15. Boren J, Cascante M, Marin S, et al. Gleevec (STI571) influences metabolic enzyme activities and glucose carbon flow toward nucleic acid and fatty acid synthesis in myeloid tumor cells. *J Biol Chem.* 2001;276(41):37747-37753. doi:10.1074/jbc.M105796200
16. Kominsky DJ, Klawitter J, Brown JL, et al. Abnormalities in glucose uptake and metabolism in imatinib-resistant human BCR-ABL-positive cells. *Clin Cancer Res.* 2009;15(10):3442-3450. doi:10.1158/1078-0432.CCR-08-3291
17. Katz JJ, Crespi HL. Isotope effects in chemical reactions. In: Collins CJ, Bowman N, eds. *Isotope Effects in Biological Systems.* Van Nostrand Reinhold; 1971:286-363.
18. Rundel PW, Ehleringer JR, Nagy KA. *Stable Isotopes in Ecological Research.* Springer; 1988.
19. Jancsó G. Isotope effects. In Vértés A, Nagy S, Klencsár Z, eds. *Handbook of Nuclear Chemistr.* Kluwer Academic Publishers; 2013: 2:85-116.
20. Somlyai G, Jancsó G, Jáklí GY, et al. Naturally occurring deuterium is essential for the normal growth rate of cells. *FEBS Lett.* 1993;317:1-4. doi:10.1016/0014-5793(93)81479-J
21. Somlyai G, Laskay G, Berkényi T, Jáklí GY, Jancsó G. Naturally occurring deuterium may have a central role in cell signalling. In: Heys JR, Melillo DG, eds. *Synthesis and Applications of Isotopically Labelled Compounds.* John Wiley and Sons; 1998: 137-141.
22. Somlyai G, Laskay G, Berkényi T, et al. The biological effects of deuterium-depleted water, a possible new tool in cancer therapy. *Zeitschrift für Onkologie (ger) Journal of Oncology.* 1998;30:91-94.
23. Cong FS, Zhang YR, Sheng HC, Ao ZH, Zhang SY, Wang JY. Deuterium-depleted water inhibits human lung carcinoma cell growth by apoptosis. *Exp Ther Med.* 2010;1(2):277-283. PMID: 22993540
24. Krempels K, Somlyai I, Somlyai G. A retrospective evaluation of the effects of deuterium depleted water consumption on four patients with brain metastases from lung cancer. *Integr Cancer Ther.* 2008;7(3):172-181. doi:10.1177/1534735408322851
25. Zhang X, Gaetani M, Chernobrovkin A, Zubarev RA. Anticancer effect of deuterium depleted water—redox disbalance leads to oxidative stress. *Mol Cell Proteomics.* 2019;18(12):2373-2387. doi:10.1074/mcp.RA119.001455
26. Zhang X, Wang J, Zubarev RA. Slight deuterium enrichment in water acts as an antioxidant: is deuterium a cell growth regulator? *Mol Cell Proteomics.* 2020;mcp.RA120.002231. doi:10.1074/mcp.RA120.002231
27. Boros LG, D'Agostino DP, Katz HE, Roth JP, Meuillet EJ, Somlyai G. Submolecular regulation of cell transformation by

- deuterium depleting water exchange reactions in the tricarboxylic acid substrate cycle. *Med Hypotheses*. 2016;87:69-74. doi:10.1016/j.mehy.2015.11.016
28. Gyöngyi Z, Somlyai G. Deuterium depletion can decrease the expression of c-myc, Ha-ras and p53 gene in carcinogen-treated mice. *In Vivo*. 2000;14:437-439. PMID: 10904878.
 29. Kovács A, Guller I, Krempels K, et al. Deuterium depletion may delay the progression of prostate cancer. *J Cancer Ther*. 2011;2:548-556. doi:10.4236/jct.2011.24075
 30. Gyöngyi Z, Budán F, Szabó I, et al. Deuterium depleted water effects on survival of lung cancer patients and expression of Kras and Bcl2 genes in mouse lung. *Nutr Cancer*. 2013;65(2):240-246. doi:10.1080/01635581.2013.756533
 31. Krempels K, Somlyai I, Gyöngyi Z, et al. A retrospective study of survival in breast cancer patients undergoing deuterium depletion in addition to conventional therapies. *J Cancer Res Ther*. 2013;1(8):194-200. doi:10.14312/2052-4994.2013-29
 32. Prosser SJ, Scrimgeour CM. High-precision determination of $^2\text{H}^1\text{H}$ in H_2 and H_2O by continuous-flow isotope ratio mass spectrometry. *Anal Chem*. 1995;67:1992-1997.
 33. Scrimgeour CM, Rollo MM, Mudambo SM, Handley LL, Prosser SJ. A simplified method for deuterium/hydrogen isotope ratio measurements on water samples of biological origin. *Biol Mass Spectrom*. 1993;22(7):383-387.
 34. Ke N, Wang X, Xu X, Abassi YA. The xCELLigence system for real-time and label-free monitoring of cell viability. *Methods Mol Biol*. 2011;740:33-43. doi:10.1007/978-1-61779-108-6_6
 35. Harrigan GG, Colca J, Szalma S, Boros LG. PNU-91325 increases fatty acid synthesis from glucose and mitochondrial long chain fatty acid degradation: a comparative tracer-based metabolomics study with rosiglitazone and pioglitazone in HepG2 cells. *Metabolomics*. 2006;2:21-29. doi:10.1007/s11306-006-0015-5
 36. Harris DM, Li L, Chen M, Lagunero FT, Go VL, Boros LG. Diverse mechanisms of growth inhibition by luteolin, resveratrol, and quercetin in MIA PaCa-2 cells: a comparative glucose tracer study with the fatty acid synthase inhibitor C75. *Metabolomics*. 2012;8(2):201-210. doi:10.1007/s11306-011-0300-9
 37. Lee WN. Stable isotopes and mass isotopomer study of fatty acid and cholesterol synthesis. A review of the MIDA approach. *Adv Exp Med Biol*. 1996;399:95-114.
 38. Lee WN, Bergner EA, Guo ZK. Mass isotopomer pattern and precursor-product relationship. *Biol Mass Spectrom*. 1992;21(2):114-122.
 39. Lee WN, Boros LG, Puigjaner J, Bassilian S, Lim S, Cascante M. Mass isotopomer study of the non-oxidative pathways of the pentose cycle with $[1,2-^{13}\text{C}_2]\text{glucose}$. *Am J Physiol*. 1998;274(5 Pt 1):E843-E851.
 40. Boros LG, Lerner MR, Morgan DL, et al. $[1,2-^{13}\text{C}_2]\text{-D-glucose}$ profiles of the serum, liver, pancreas, and DMBA-induced pancreatic tumors of rats. *Pancreas*. 2005;31(4):337-343. PMID: 16258367
 41. Addeo P, Oussoultzoglou E, Fuchshuber P, et al. Safety and outcome of combined liver and pancreatic resections. *Br J Surg*. 2014;101(6):693-700. doi:10.1002/bjs.9443
 42. Lin WC, Rajbhandari N, Wagner KU. Cancer cell dormancy in novel mouse models for reversible pancreatic cancer: a lingering challenge in the development of targeted therapies. *Cancer Res*. 2014;74(8):2138-2143. doi:10.1158/0008-5472.CAN-13-3437
 43. Cantoria MJ, Boros LG, Meillet EJ. Contextual inhibition of fatty acid synthesis by metformin involves glucose-derived acetyl-CoA and cholesterol in pancreatic tumor cells. *Metabolomics*. 2014;10:91-104. doi:10.1007/s11306-013-0555-4
 44. Hao D, Sarfaraz OM, Farshidfar F, et al. Temporal characterization of serum metabolite signatures in lung cancer patients undergoing treatment. *Metabolomics*. 2016;12. doi:10.1007/s11306-016-1068-8
 45. Gros SJ, Holland-Cunz SJ, Supuran CT, Braissant O. Personalized treatment response assessment for rare childhood tumors using microcalorimetry—exemplified by use of carbonic anhydrase IX and aquaporin 1 inhibitors. *Int J Mol Sci*. 2019;20(20):4984. doi:10.3390/ijms20204984
 46. Pandei N, Lanke V, Vinod PK. Network-based metabolic characterization of renal cell carcinoma. *Sci Rep*. 2020;10(1):5955. <https://www.nature.com/articles/s41598-020-62853-8>
 47. Arima K, Lau MC, Zhao M, et al. Metabolic profiling of formalin-fixed paraffin-embedded tissues discriminates normal colon from colorectal cancer. *Mol Cancer Res*. 2020;18(6):883-890. doi:10.1158/1541-7786.MCR-19-1091
 48. Boros LG, Collins TQ, Somlyai G. What to eat or what not to eat—that is still the question. *Neuro-Oncology*. 2017;19(4):595-596. doi:10.1093/neuonc/now284
 49. Kuroda T, Kumagi T, Yokota T, et al. EPOCH-Study-Group. Improvement of long-term outcomes in pancreatic cancer and its associated factors within the gemcitabine era: a collaborative retrospective multicenter clinical review of 1,082 patients. *BMC Gastroenterol*. 2013;13:134. doi:10.1186/1471-230X-13-134
 50. Von Hoff DD, Erwin T, Arena FP, et al. Increased survival in pancreatic cancer with nab-paclitaxel plus gemcitabine. *N Engl J Med*. 2013;369(18):1691-1703. doi:10.1056/NEJMoa1304369
 51. Tedeschi PM, Markert EK, Gounder M, et al. Contribution of serine, folate and glycine metabolism to the ATP, NADPH and purine requirements of cancer cells. *Cell Death Dis*. 2013;4:e877. doi:10.1038/cddis.2013.393
 52. Boros LG, Collins TQ, Boros EA, Lantos F, Somlyai G. Deuterium and metabolic water matter—what this means biochemically and clinically. eLetter Comment on: De Feyter, HM, Behar, KL, Corbin, ZA, Fulbright, RK, Brown, PB, McIntyre, S, Nixon, TW, Rothman, DL, Robin A. de Graaf, RA. Deuterium metabolic imaging (DMI) for MRI-based 3D mapping of metabolism in vivo. *Sci Adv*. 2018;4(8):eaat7314. doi:10.1126/sciadv.aat7314